Available online at www.sciencedirect.com
SCIENCE DIRECT
Polymer 46 (2005) 10128–10138
polymer
www.elsevier.com/locate/polymer

A Monte Carlo simulation study of the mechanical and conformational properties of networks of helical polymers. Part II. The effect of temperature

Richard Batman, Gustavo A. Carri*

Department of Polymer Science and The Maurice Morton Institute of Polymer Science, The University of Akron, Akron, OH 44325-3909, USA

Received 30 May 2005; received in revised form 30 July 2005; accepted 3 August 2005
Available online 19 August 2005

Abstract

In a recent article (Carri GA, Batman R, Varshney V, Dirama TE. Polymer 2005;46:3809 [17]) we presented a model for networks of helical polymers. In this article we generalize our results to include the effect of temperature and focus on the mechanical, conformational and thermo-elastic properties of the network. We find that the non-monotonic stress–strain behavior observed at constant temperature also appears in the stress–temperature behavior at constant strain. The origin of this behavior is traced to the induction and melting of helical beads by the application of large strains or reduction in temperature. Other conformational properties of the polymer strands are also discussed. We also study the network entropy and heat capacity, and find a non-monotonic dependence on temperature and strain. Our study shows that the entropy is controlled by the helical content whenever the latter is significant. Otherwise, the entropy corresponds to the one of a network made of random coils. In addition, the study of the heat capacity shows that strain shifts the helix-coil transition temperature significantly. Other results are also discussed.

Keywords: Networks; Elastomers; Helical polymers

1. Introduction

The large deformability and almost complete recoverability of elastomers have made them objects of scientific study for several decades. As in the first experiments of Gough and Joule [1,2] testing has generally involved the measurement of mechanical stress corresponding to some sort of strain, most often uniaxial extension or compression. Additional information relating mechanical properties to molecular structure has been obtained from a variety of experimental techniques including swelling experiments, NMR, SAXS, SANS and others [3].

Experimental studies have shown that elastomers consist of macromolecular chains, cross-linked into a network, that can change their conformations in response to stress. Theories based on this model, described in a recent review by Erman and Mark [4], simplified the calculations by making various assumptions. In the earliest theories [2,5,6] the network strands were treated as perfectly flexible 'phantom chains' that passed freely through each other, interacting only at cross-links. In such networks, the stress arises from the decrease in the entropy of the network chains due to the deformation. Interactions between strands were incorporated into later theories [7].

Computer simulations have generally followed two different methods in studying elastomers. The more direct method of modeling the fully-constructed network is exemplified in the work of Grest and Kremer, and Escobedo and de Pablo [8,9]. The less direct but more common method is the Monte Carlo modeling of a single, isolated chain to obtain the radial distribution function of end-to-end distance, which is then used in the standard three-chain model of rubberlike elasticity to find the stress–strain behavior of the network [2,6]. This method has been extensively used with synthetic systems [4].

Most of the studies have focused on synthetic elastomers. However, biopolymers are richer in terms of their conformational properties; thus, networks made of

* Corresponding author. Tel.: +1 330 972 7509; fax: +1 330 972 5290.
E-mail address: gac@uakron.edu (G.A. Carri).

0032-3861/$ - see front matter © 2005 Elsevier Ltd. All rights reserved.
doi:10.1016/j.polymer.2005.08.013

biopolymers, called bioelastomers, can be expected to have a more interesting stress–strain behavior. The secondary structures of biopolymers, such as α-helices and β-sheets, as well as their tertiary structures, can be melted at sufficiently high temperatures or pulled apart by sufficiently large strains. These structures would therefore produce significant temperature- and strain-dependence in the mechanical properties of networks. The presence of solvent, which also affects the formation and melting of such structures, would add a further dimension to the behavior of swelled networks.

In order to take full advantage of the potential of novel bioelastomers, much work remains to be done. Indeed, there are very few studies of bioelastomers such as elastin and resilin [4,10]. In general, the investigation of biopolymer mechanics has largely been restricted to single-chain elasticity experiments. These have been greatly encouraged by the recent development of single molecule force spectroscopy (SMFS) which has been applied to RNA and DNA, the polysaccharides dextran and xanthan, the muscle protein Titin, and various other bio- and synthetic polymers [11].

Researchers are already beginning to build new materials from biopolymers [12], in the hope of harnessing the endless variety and complexity of their behavior, which has motivated the modeling work in this article. Our method follows the common scheme in which the simulation of a single chain generates the radial distribution function, which we use as input in the Three-chain model. We describe the helical polymer using a model recently developed by us [13]. The study of helical polymers, which exist in a helical conformation at low temperature and melt into a random-coil conformation in response to an increase in temperature or a change in solvent quality [13,14], will allow us to focus on the simplest of secondary structures, the α-helix. The transition described above produces a complex mechanical behavior that changes at around the transition temperature of a single chain. We will also compare our simulation results to the theoretical ones of Kutter and Terentjev for networks of helix-forming polymers [15].

The Monte Carlo algorithm of Wang and Landau [16] is used to simulate the homopolypeptide chain. The simulation results, in conjunction with the three-chain model, will be used to calculate the stress–strain behavior of the network, as well as the conformational properties of the constituent chains for different temperatures and degrees of strain.

This article is organized as follows. In the second section, we briefly describe our simulation protocol and the three-chain model. In the third section, we present our results for the stress–strain and thermo-elastic behavior of the network and single chain, and rationalize the effect of temperature and strain on various equilibrium properties, including the entropy of the network. Finally, we conclude the present article by summarizing the most important findings of our work and with the appropriate acknowledgements.

2. Simulation protocol and theoretical model

2.1. Model and simulation methodology

The helical polymer was modeled using the freely rotating chain model, in which each bead represents an amino acid residue. The interactions between pairs of beads were modeled with a hardcore potential energy, and the tendency toward the helical conformation was modeled using a criterion based on the concept of torsion of a curve [13,17]. Each bead that satisfied this criterion was considered to have a helical conformation and was assigned a negative enthalpy called C, which stabilizes the helical conformation. Otherwise, the bead was considered to have a random coil conformation, which was used as the reference state. We chose $C=-1300$ K, so that the helix-coil transition temperature is close to 300 K. These concepts were implemented in a Monte Carlo simulation based on the Wang–Landau algorithm [16]. The outcome of this procedure is the density of states, which we used to compute the free energy and radial distribution function of the polymer [17]. The latter is the input required by the three-chain model of rubberlike elasticity. More details about the simulation protocol and model employed can be found in Ref. [17].

2.2. The three-chain model

The three-chain model assumes that inter-chain interactions are independent of deformation and averages the free energies of three chains oriented in three orthogonal orientations, which are deformed in the affine limit at constant volume. The macroscopic deformations of the network are $\lambda_i=L_i/L_{i0}$, where L_i and L_{i0} indicate the deformed and undeformed dimensions of the network in the ith direction, respectively. For uniaxial extension the conservation of volume implies that $\lambda_x=\lambda, \lambda_y=\lambda_z=\lambda^{-1/2}$. Thus, the total free energy of a network made of ϕ chains per unit volume relative to the unstrained state is given by the equation

$$\Delta f_{\text{net}} = \phi\left(\frac{f(R_0\lambda)}{3}+\frac{2f(R_0\lambda^{-1/2})}{3}-f(R_0)\right) \tag{1}$$

R_0 is the average end-to-end distance of a chain in the undeformed state and $f(x)$ is the free energy (in units of Boltzmann's constant, k_B) of a single chain with end-to-end distance x. $f(x)$ is obtained from $f(x)=\Delta f(x)+F(T)$ where $F(T)$ is the free energy of a chain, independent of x [13] and $\Delta f(x)$ is the free energy (relative to the free chain) of a chain with end-to-end distance equal to x. The latter is given by $\Delta f(x)=-T\ln(W(x))$, where $W(x)$ is the probability distribution of the end-to-end distance obtained from the Monte Carlo simulation. Differentiating Eq. (1) with respect to λ at constant temperature gives the nominal stress of the network

$$\sigma' = \frac{\phi R_0}{3}(F(R_0\lambda) - \lambda^{-3/2}F(R_0\lambda^{-1/2})) \quad (2)$$

where $F(x)$ is the retraction force of a single chain

$$F(x) = \left(\frac{\partial(\Delta f(x))}{\partial x}\right)_T \quad (3)$$

The total entropy of the network relative to the unstrained state is given by

$$\Delta S_{\text{net}} = \phi\left(\frac{S(R_0\lambda)}{3} + \frac{2S(R_0\lambda^{-1/2})}{3} - S(R_0)\right) \quad (4)$$

where $S(x)$ is the single-chain entropy in units of k_B. The latter is obtained from

$$S(x) = \Delta S(x) + S(T) \quad (5)$$

where $\Delta S(x) = -(\partial(\Delta f(x))/\partial T)_x$ is the entropy (relative to the free chain) of a chain with end-to-end distance equal to x, and $S(T)$ is the entropy of a free chain [13]. Finally, the heat capacity of the network relative to the unstrained state is

$$\Delta(C_v)_{\text{net}} = \phi\left(\frac{C_v(R_0\lambda)}{3} + \frac{2C_v(R_0\lambda^{-1/2})}{3} - C_v(R_0)\right) \quad (6)$$

where $C_v(x)$ is the single-chain heat capacity in units of k_B and is obtained from

$$C_v(x) = T\left(\frac{\partial(\Delta S(x))}{\partial T}\right)_x + C_v^S(T) \quad (7)$$

where $C_v^S(T)$ is the heat capacity of a free chain [13].

3. Results and discussion

Fig. 1 shows the radial distribution function of a single chain with 30 beads, $g(R)$, as a function of the end-to-end distance, R, and temperature, T. The helix-coil transition temperature, T_{hc}, is 311 K and is mainly determined by the parameter $C(=-1300\text{ K})$ of the model. Therefore, the range of temperatures shown (200–500 K) covers all possible behaviors of the chain from the helical structure at low temperatures to the random coil conformation at high temperatures. Fig. 1 shows that as T decreases, the peak in $g(R)$ shifts towards larger values of R due to the formation of helical sequences, which make the chain stiffer. This shift occurs around T_{hc}. Careful examination shows that the single peak present at 200 K splits into two peaks at slightly higher temperatures, leading to a multimodal distribution, which agrees with previous studies on poly(oxymethylene) [18]. POM is known to adopt the helical conformation under some conditions. At high temperatures the peak occurs at smaller values of R and is broader than at low temperatures due to the absence of helical sequences.

Fig. 2 shows the retraction force of the chain, F, as a function of R and T. F increases monotonically with increasing R at high T, as expected for a random coil. However, as T decreases below T_{hc} and the tendency to form helical strands increases, F becomes a non-monotonic function of R, first increasing and then decreasing before a final increase to very high values at the fully extended length of the chain. The behavior of F is related to the helical content, θ (Fig. 3), which increases with decreasing T. However, its dependence on R is more complex. At a given temperature, θ first increases as the chain is stretched due to induction of helices by the external force [13]. This increase continues until the helices are pulled apart, i.e. until R becomes too large to allow helical sequences to remain intact. Upon further extension, θ decreases to zero at the fully extended length of the chain. When plotting θ as a function of R for various (constant) values of T, the peaks in all the curves occur at the same value of R ($=31$, approximately). This is roughly the same value of R at which F exhibits its first sudden increase in Fig. 2. Thus, at low temperatures, the non-monotonic dependence of F on R is related to the unraveling of helices. If we now look at θ as

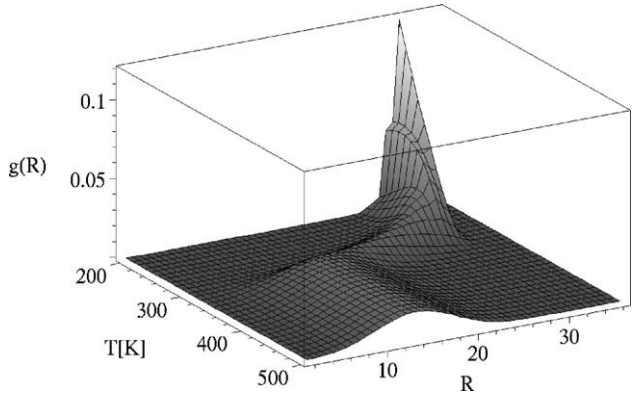

Fig. 1. Radial distribution function as a function of the end-to-end distance and temperature for a chain with 30 beads. The position of the peak shifts towards larger values of the end-to-end distance at the helix-coil transition temperature.

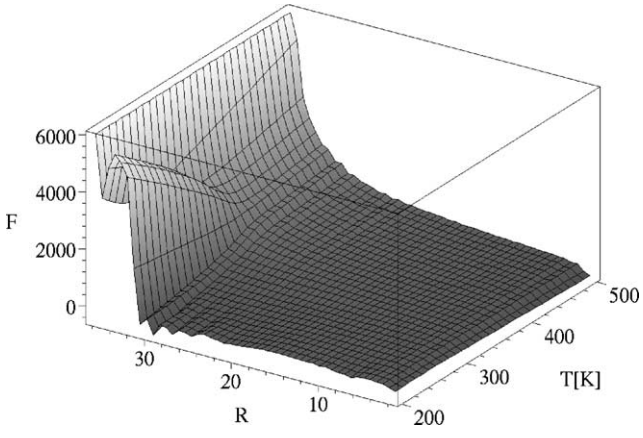

Fig. 2. Retraction force as a function of the end-to-end distance and temperature for a chain with 30 beads. The dependence on end-to-end distance becomes non-monotonic below the helix-coil transition temperature.

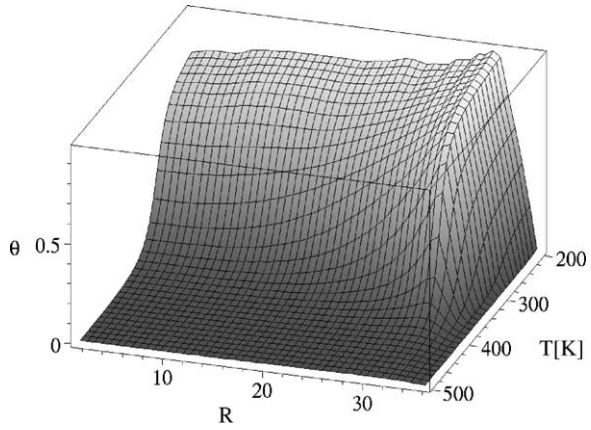

Fig. 3. Helical content as a function of the end-to-end distance and temperature for a chain with 30 beads. The helical content increases with decreasing temperature for all values of end-to-end distance and decreases to zero for values of the end-to-end distance larger than the end-to-end distance of the full helix.

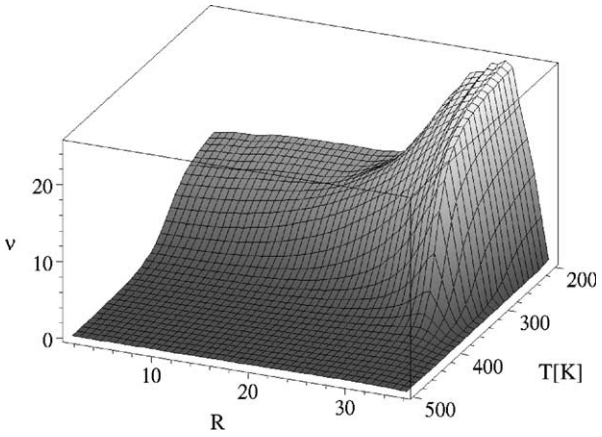

Fig. 4. Average number of beads per helical strand as a function of the end-to-end distance and temperature for a chain with 30 beads. At low temperatures, when R is close to 25, ν changes from 15 to 25, signaling the formation of longer helical strands.

a function of T for fixed values of R, the typical sigmoid-like shape is observed. However, T_{hc} increases with increasing values of R until, of course, it disappears when the degree of stretching does not allow the formation of helical strands. This behavior is simple to understand. At low temperatures, values of R smaller than the equilibrium value, which corresponds to the perfect helix, force the helix to break into two helical strands. These strands are shorter than the full helix; consequently they are less stable in the thermodynamic sense. Therefore, less thermal energy is required to melt them and T_{hc} decreases. Increasing R reduces the constraint, longer helical strands are compatible with the constraint and do form. Since the helices are longer, they are more stable; thus, T_{hc} increases. However, as soon as R becomes larger than the end-to-end distance of the helix, then the length of the helical strands starts to decrease. Therefore, these strands become less stable and T_{hc} decreases.

The molecular mechanisms responsible for the behavior of θ can be clarified by examining the average number of beads per helical strand (ν) and the average number of helical strands in the chain (μ). Fig. 4 shows ν as a function of R and T. Although the increase at large end-to-end distance is more pronounced than for θ, the basic trends are the same. Comparing the constant-temperature cross-sections of ν with those of θ (not shown) reveals the same pattern at all temperatures: ν increases with increasing R until the latter reaches a value close to 31, and then decreases to zero rapidly. The plot of μ as a function of R and T in Fig. 5 shows a similar behavior at high temperatures. In this regime, μ and ν increase and decrease simultaneously; thus, the helical content must increase by nucleation and growth of short helical strands that rarely merge together, and decrease by unraveling of these strands from the ends. Below T_{hc}, μ decreases monotonically with increasing R. First, μ stays roughly constant at a value of about 2 for small values of R, and then, when $R \approx 25$, it drops to a second plateau where it remains roughly constant at a value of 1. This drop occurs when ν is approximately 15 (half the number of beads in the chain). What is happening is easy to understand. For small values of R the helix is broken in two shorter helical strands that are parallel to each other. Increasing the value of R relaxes this constraint; thus, more conformations can be explored. At $R \approx 25$ the constraint is such that the chain can form one long helical strand (although it is not a complete helix). Thus, μ decreases from 2 to 1 and ν increases from 15 to about 25. For values of R larger than the end-to-end distance of the helix, ν decreases rapidly while μ remains constant until dropping discontinuously to zero at full extension. This indicates that the single helical strand unravels from the ends.

The entropy of a single chain, S, is plotted as a function of R and T in Fig. 6. It is controlled by θ wherever the latter

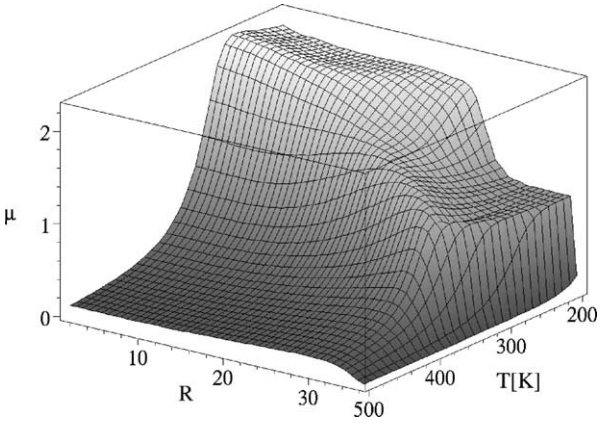

Fig. 5. Average number of helical domains as a function of the end-to-end distance and temperature for a chain with 30 beads. The step-like decrease from two domains to one as the end-to-end distance increases below the helix-coil transition temperature signals the reunification of two domains, which occurs at the same value of R where ν increases from 15 to 25 in Fig. 4.

is significant, since the formation of a helix reduces the number of configurations available to the chain. At very low temperatures, S decreases with increasing R due to the increase of the helical content. When R reaches the value at which the helix starts to unravel, S begins to increase rapidly due to the interconversion of helical beads into coil beads, which have higher configurational entropy. On the other hand, at high temperatures, S decreases monotonically, as one would expect for a random coil. In addition, a detailed analysis of the plot shows a sudden decrease in S at full extension caused by the stretching of the random coil after all helical strands have completely unwound. Some small negative values of S are seen at large values of R, which we ascribe to increased statistical error in this region. Also, if R is kept constant, Fig. 6 shows that S increases with increasing temperature except in the region where increased statistical error is observed ($R \sim 31$).

Fig. 7 shows the heat capacity, C_v, of a single chain as a function of R and T. C_v is expected to reach a peak at T_{hc}. As is seen in Fig. 7, T_{hc} and the sharpness of the transition increase with increasing R. C_v exhibits a ridge that runs slightly off-parallel to the R axis in the mid-range of temperatures. As R increases from 0 to about 31, T_{hc} shifts from 300 to 350 K, and the sharpness of the peak increases. Close examination shows that, when R exceeds 31 and the proximity to the full extension begins to unwind the helices, the peak suddenly shifts to lower temperatures in agreement with the fact that shorter helical strands are less thermodynamically stable. The dependence of the sharpness and location of the transition on R can be explained using simple physical concepts. If R is small, then the polymer strand forms two parallel, short helices. Since they are shorter than the complete helix, T_{hc} should be lower and the width of the transition should be broader than for the complete helix [13]. As R increases, longer helical strands can form, which shifts T_{hc} to higher temperatures and makes

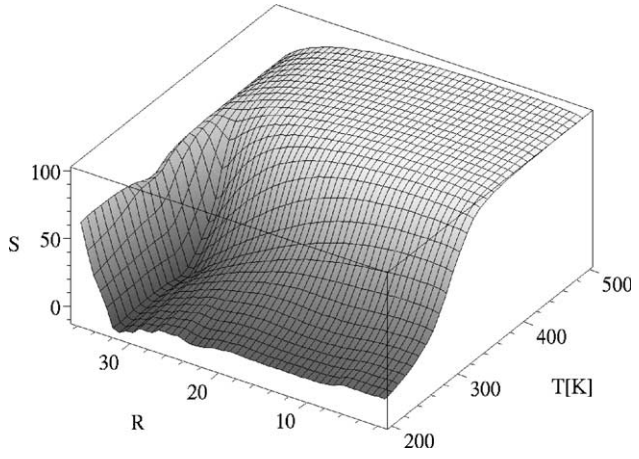

Fig. 6. Entropy as a function of the end-to-end distance and temperature for a chain with 30 beads. The non-monotonic dependence on end-to-end distance below the helix-coil transition temperature results from the induction and melting of helices by elongation.

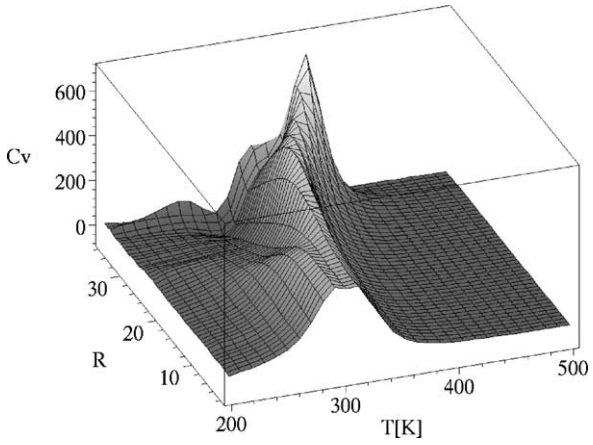

Fig. 7. Heat capacity as a function of the end-to-end distance and temperature for a chain with 30 beads. The shift of the position of the peak to higher temperature as end-to-end distance increases results from the increased helix-coil transition temperature associated with the formation of longer and more thermally stable helical domains.

the transition narrower [13] until the extension of the chain is too large and the helix breaks apart, leaving short helical strands and random coil domains. The presence of short helices shifts T_{hc} back to lower temperatures, as observed in our simulation study.

Fig. 8(a) shows the stress of the network as a function of the strain, λ, and T for the cases of uniaxial extension and compression. The quantity plotted is $\sigma^* = 3\sigma'/\phi R_0$, where σ' is the nominal stress. As the temperature decreases below T_{hc}, the range of allowed strain narrows due to the increase in R_0 and the finite extensibility of the chain. In addition, the dependence of σ^* on λ at constant T changes from a monotonic increase with increasing λ to a non-monotonic, more complex behavior similar to the one observed in Fig. 2. Let us elaborate this point. We start by analyzing σ^* for the case of simple extension ($\lambda > 1$). For all the cases studied, σ^* increases with increasing λ, as expected. However, the physical origins of this increase are more complex than in the case of simple synthetic polymers. Indeed, there are two kinds of forces resisting the deformation of the network: the decrease in the entropy of the system, which is also present in synthetic elastomers and can be described using classical theories of rubber elasticity, and the formation of helical strands, which is known to be facilitated by the application of external mechanical forces [13]. Fig. 8(b) shows cross-sections of Fig. 8(a) that show the dependence of σ^* on λ at 200, 250, 300, 350 and 400 K. Let us examine the curves for temperatures below T_{hc}: 200, 250 and 300 K. σ^* first increases with increasing λ, indicating that the network gets stronger as we stretch it, then decreases which points to a softening of the network before a final, sharp increase to very high values due to the finite extensibility of the polymer strands. At temperatures above T_{hc} the softening of the network is not observed, i.e. σ^* always increases with increasing λ. However, at 350 K, a clear 'shoulder' is observed before the final increase of σ^*.

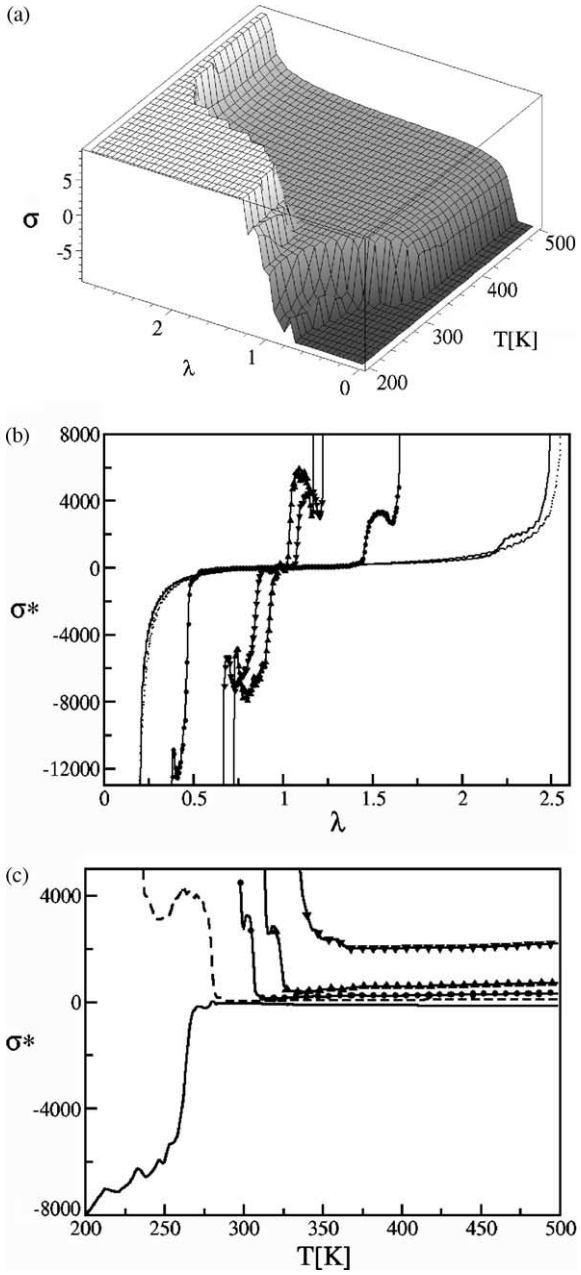

Fig. 8. (a) Rescaled stress (σ^*) (in thousands) as a function of λ and temperature. (b) Constant-temperature cross-sections. (▲) 200 K, (▼) 250 K, (●) 300 K, (line) 350 K, (dots) 400 K. (c) Rescaled stress (σ^*) as a function of temperature for various values of λ. (line) 0.8, (dashed line) 1.2, (●) 1.6, (▲) 2.0, (▼) 2.4. The non-monotonic stress–strain behavior, which is not observed in synthetic elastomers, appears at temperatures below the helix-coil transition temperature. The non-monotonic thermo-elastic behavior is also shown.

The 'shoulder' does not appear at 400 K, since virtually no helical strands are present at this temperature prior to stretching. Thus, the origin of the decrease in σ^* for temperatures below T_{hc} is directly related to the presence of helical strands before the network is stretched.

Under uniaxial compression ($\lambda < 1$), which is equivalent to biaxial extension in the orthogonal directions, the system displays behavior that is similar to that associated with uniaxial extension that can be rationalized using the same arguments presented above. The only difference is that σ^* is negative, which indicates that the system is under compression.

Fig. 8(c) shows the thermo-elastic behavior of the network for values of λ equal to 0.8, 1.2, 1.6, 2 and 2.4. In the case of uniaxial elongation and for T above T_{hc}, σ^* increases with increasing T, as expected for a network of random coils. The rise in T increases the entropy of the system, thus strengthening the retraction forces present in the network. However, if T is decreased and crosses T_{hc}, enthalpy starts to favor the formation of helical strands. Thus, in order to impose the strain on the network, more force has to be applied to overcome the tendency of the system to form helices. Consequently, σ^* increases with decreasing T. The temperature at which the first increase in σ^* occurs is the same temperature at which θ and ν reach a maximum, but μ is larger than one implying that short helices are present in the network. A further decrease in T shows a decrease in the stress until a minimum is reached. Beyond this point, the stress increases rapidly. The existence of a minimum can be understood using basic physical concepts. As T is reduced, the tendency of enthalpy to favor the formation of one long helical strand increases [13]. However, the applied strain puts a constraint on the end-to-end distance. As a consequence of these two conditions, the average polymer strand forms only one helical strand, which is shorter than at slightly higher temperatures, and melts the short helices to satisfy the geometric constraint imposed by the applied strain. Thus, more beads adopt the random coil conformation, making the chain more flexible, and, consequently, σ^* decreases. However, further decrease of T strengthens the tendency to form long helical sequences; therefore, more force has to be applied to keep the applied strain constant, i.e. σ^* increases. These results are illustrated in Fig. 9, where we plot σ^*, θ and μ on the same plot for $\lambda = 1.2$. The dependence of θ and ν on T are the same as can be observed from Figs. 10(a) and 11. Observe that for $\lambda = 2.4$ the softening of the network is not observed in Fig. 8(c). For this value of λ, the deformation is so large that helical sequences do not form. However, the enthalpic driving force is present; thus, σ^* increases as T is reduced. The behavior of σ^* for the case of compression, $\lambda < 1$, can be understood using similar arguments.

Fig. 10(a) shows θ as a function of λ and T. Below T_{hc}, θ decreases monotonically with increasing or decreasing λ, while, above T_{hc}, it first increases before dropping at large λ. Specifically, at low temperatures θ is high. For example, at 250 K the value is close to 0.9, indicating that 90% of the beads are in the helical conformation. Observe that this value remains constant until it starts to decrease for values of λ larger than $\lambda_0(T)$. In the case of 250 K, the value of $\lambda_0 = 1.15$. This implies that extension ratios larger than 1.15 interfere with the formation of helical strands, i.e. the elongation of the network is too large for the formation of helical strands, or, in other words, the polymer strands are

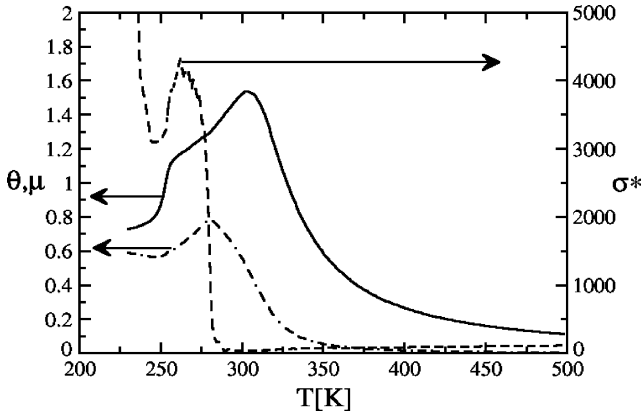

Fig. 9. σ^* (Dashed line), μ (continuous line) and θ (double dashed-dotted line) as functions of temperature for $\lambda = 1.2$. The first sharp increase of the stress with decreasing temperature is caused by an increase in the helical content of the chain, where many helical strands are present. The minimum occurs when all the helical strands merge into a long one. The large increase at lower temperatures is a consequence of stretching one long and thermodynamically stable helical strand.

overstretched with respect to the end-to-end distance of the helix. Therefore, an increasing number of segments adopt the random coil conformation to satisfy the constraint

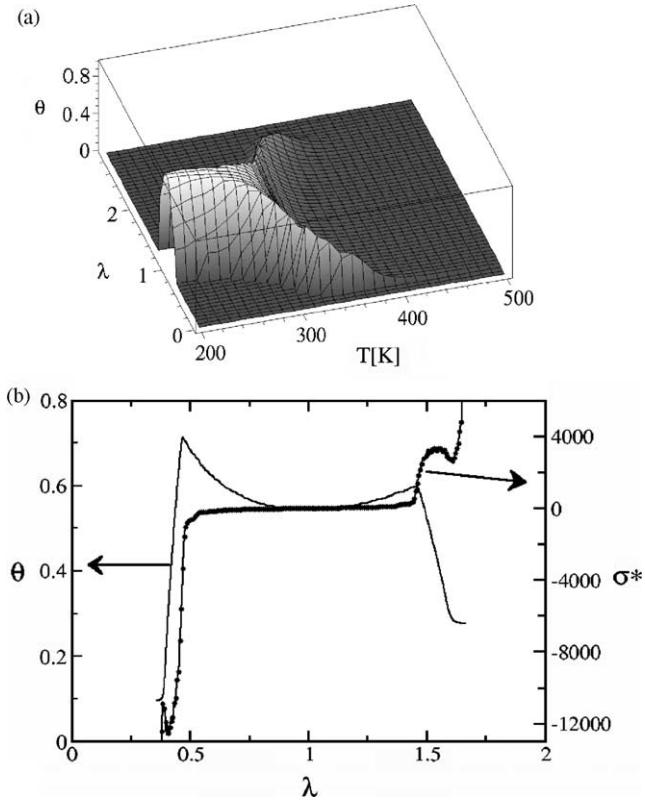

Fig. 10. (a) Helical content as a function of λ and temperature. (b) Helical content (line) and rescaled stress, σ^*, (●) as functions of λ at 300 K. The sharp increase in stress coincides with the peak in helical content, indicating that helices are being torn apart. This requires more energy than stretching random-coil segments; thus, the stress increases. The subsequent drop in stress is caused by a rise in entropy associated with the decrease in helical content.

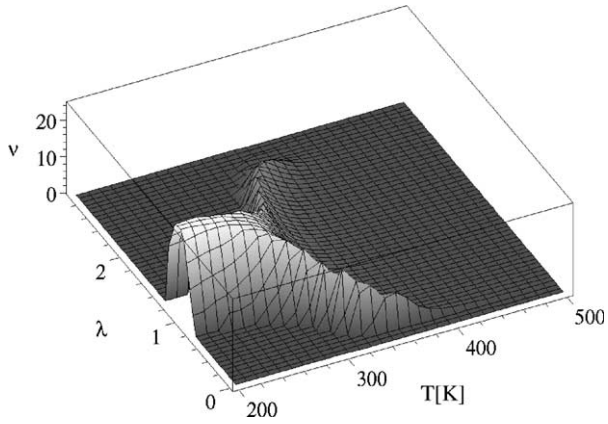

Fig. 11. Average number of beads per helical strand as a function of λ and temperature.

imposed by the deformation. Consequently, θ decreases. It is important to note that this behavior of θ predicted by our simulation study was also predicted by the theoretical calculations of Kutter and Terentjev (Fig. 10 in Ref. [15]). However, they used the Gaussian distribution for the description of flexible coils, which did not allow us to carry out a quantitative comparison between theory and simulations. Nevertheless, the results agree on a qualitative level. At higher temperatures, e.g. 350 K, the behavior of θ is different. Indeed, upon the extension of the network θ first increases and then decreases in qualitative agreement with the results of Kutter and Terentjev (Fig. 9 in Ref. [15]). The initial increase of θ indicates that the application of an external mechanical force first stabilizes the helical conformation. This increase of θ can be achieved in two ways: first, the helical strands could be longer, i.e. more beads per strand, and, second, more helical strands could be formed. A further increase of the extension ratio interferes with the formation of helices and θ decreases.

If λ is held constant, then, as T decreases from 500 K for each value of strain, θ increases monotonically until it reaches a maximum and then decreases to zero. The only exception occurs for values of λ very close to 1. This increase in θ with decreasing T is due to the tendency of the system to form helices at low temperatures. A further decrease of T increases the end-to-end distance of the average polymer strand [13], which becomes slightly shorter than that of the fully extended conformation. Thus, θ approaches zero with decreasing temperature for any value of $\lambda \geq L_{\text{extended}}/L_{\text{helix}}$; otherwise, the strands would be overstretched with respect to the fully extended conformation, a result that is not physical. L_{helix} and L_{extended} are the end-to-end distance of the helix and fully extended conformation, respectively. In addition, Fig. 10(a) shows that the peak in θ occurs at higher values of T for larger values of λ. This is the consequence of the stabilization of the helical conformation by the deformation, as discussed before for the case of the single chain. A more stable helical structure requires more thermal energy to melt it.

Using the results obtained for θ and σ^*, we can now provide an explanation for the physical origins of the stress–strain behavior (which, by analogy, also applies to the force-extension behavior of a single chain in Fig. 2). For this purpose, we combined the data for σ^* and θ at 300 K in one plot, Fig. 10(b). Observe that for values of λ slightly above 1 both σ^* and θ increase. This implies that more and/or longer helical strands are formed as we stretch the network. We discuss this point below. The formation of new helical strands and/or the increase of the length of the helical strands decreases the entropy of the system because it removes many rotational degrees of freedom from the polymers. Thus, the decrease of the entropy of the network is faster than in the typical case of synthetic polymers (i.e. without secondary structures) and, moreover, has two contributions: first, the loss of entropy due to the elongation of the random coil segments and, second, the loss of random coil segments due to the stabilization of the helical conformation by the external mechanical force.

Fig. 10(b) also shows that when θ is about to reach its maximum, σ^* increases abruptly. The sharp increase in σ^* implies that, for this particular value of λ, the polymer strands are almost completely aligned parallel to the stretching force, and all the random coil segments are almost fully stretched. Consequently, the external force is resisted by the helical strands. Since these strands are more stable due to the molecular driving forces that stabilize the helical conformation (e.g. hydrogen bonds), more force is required to overcome this thermodynamic barrier and melt the helices. Consequently, σ^* increases. Upon further increase of λ, the network overcomes the thermodynamic barrier, and fewer and shorter helices remain. Consequently, the number of segments in the random coil conformation increases, which, in turn, increases the entropy of the network. Thus, the network softens and σ^* decreases. Finally, for very large deformations, the polymer strands are fully stretched and σ^* diverges to infinity.

The previous rationalization of the stress–strain behavior at 300 K is also valid for 350 K. However, the behavior at 250 K is slightly different. Indeed, θ (Fig. 10(a)) remains approximately constant while σ^* increases, Fig. 8(a). This implies that even for small values of λ the external force is resisted by the helical strands. This is to be expected because 90% of the beads are in the helical conformation. A similar behavior is seen at 200 K.

In order to understand the behavior of the helical content, we plot the average length of a helical strand, ν, and the average number of helical strands, μ, as functions of λ and T in Figs. 11 and 12, respectively. Comparison of Fig. 11 with Fig. 10(a) shows that ν follows the same behavior as θ. Comparison of Fig. 10(a) with Fig. 12, however, shows that, near T_{hc}, increasing θ decreases μ and vice versa. This will be discussed in detail below. Cross-sections of the plots in Figs. 11 and 12 show that at 250 K both ν and μ are approximately constant until they decrease sharply for values of λ larger than 1.15. Thus, the behavior of θ follows

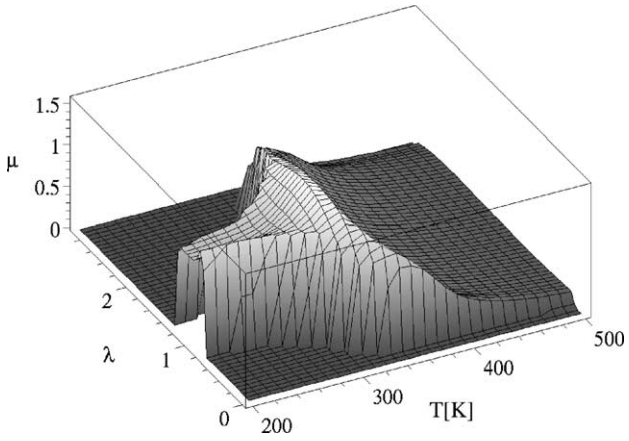

Fig. 12. Number of helical strands as a function of λ and temperature.

the ones of ν and μ. These results indicate that the mechanism leading to the decrease of θ with increasing values of λ involves helical strands unwinding from the ends. At 300 K, the situation is different. μ Decreases with increasing λ, which implies that the deformation decreases the average number of helical strands; however, ν increases. Eventually, ν overrides the decrease of μ and θ increases. These results suggest that the deformation of the network tends to merge the helical strands into longer and thermodynamically more stable ones. Again, for large deformations the helical strands unwind from the ends. Finally, the situation changes again at 350 K. In this case both ν and μ increase with increasing λ. This leads to a substantial increase in the helical content by a factor of 5 when $\lambda \approx 2.4$ and indicates that the deformation of the network stabilizes helical strands of any length.

Cross-sections of Figs. 10(a) and 11 show that ν has the same temperature dependence of θ, both having coincident peaks. ν and μ show similar dependences on T and no significant differences between the positions of peaks for λ values equal to 1.6 and 2.0. This indicates that, for such strains, the formation and melting of helices involve winding to, or unwinding from, the ends of helical domains, rather than the breaking up or merging of sequences. However, at a strain of 1.2, θ and ν begin dropping from their peaks at about 280 K, while μ continues to rise to a later peak at about 303 K. This indicates that, at smaller strains, the decrease in θ with increasing T originates from breaking longer sequences into shorter ones.

Let us now rationalize the results obtained for the case of compression ($\lambda < 1$) briefly. In this case, the network is compressed in one direction. Consequently, it is stretched in the two orthogonal directions, because the volume must be conserved in the three-chain model. Thus, all the results reported for the case of uniaxial extension, like the increase in θ and ν with increasing λ, etc. should also appear in compression for decreasing values of λ. This is what all the plots show. The only difference is that σ^* is now negative, indicating that the system is under compression. However,

all the other features observed for the case of uniaxial extension are present and can be rationalized using arguments similar to those employed to understand the effect of uniaxial elongation.

We now consider the entropy of the network, S. Fig. 13 shows S as a function of λ and T. More specifically, what is plotted is the change in entropy ($\Delta S_{net}/\phi k_B$), where the reference state is the unstrained network. S depends mainly on θ, generally decreasing as the latter increases and vice-versa, so that the entropy plot is somewhat similar to Fig. 10(a) turned upside-down. Three regimes can be identified in Fig. 13. At high temperatures, a compression or an extension of the network decreases S. This is the expected behavior for a network made of random coils because the strain stretches the coils, thus reducing their entropy. At temperatures close to T_{hc}, an increase in λ first decreases the entropy. There are two driving forces for this. First, the random coils are stretched, so their entropy decreases. Second, the force stabilizes the helical conformation. Thus, more beads adopt the helical conformation, which carries a lower entropy. However, further increase of λ disrupts the formation of helical sequences, and many beads adopt the random coil conformation. This increases S, as shown in Fig. 13. Further extension forces the polymer strands into their fully extended conformations; thus, S decreases. At low temperatures, most of the system is in the helical state; thus, the deformation of the network reduces θ. Consequently, more beads become random coils and S increases.

Two regimes can be observed in Fig. 13 when λ is held constant. For large strains (e.g. $\lambda=1.5$) and decreasing temperatures S first decreases and then increases. The decrease is a consequence of the tendency of the polymer strands to adopt the helical conformation at low temperatures, which reduces S. Moreover, the application of strain facilitates the formation of helices, which results in a decrease of ΔS at higher temperatures. Upon further decrease in temperature, the strands try to form long helical structures. However, the degree of deformation does not allow the formation of complete helices; thus, short helices are melted to accommodate the imposed strain and the enthalpic preference for long helical strands. This increase in the number of beads in the random coils increases S. Further reduction of the temperature forces the polymer strands into their fully extended conformation, and S decreases. This behavior is valid for values of $\lambda \geq L_{extended}/L_{helix}$. For values of λ between 1 and $L_{extended}/L_{helix}$, the strain is not large enough to facilitate the formation of helices in a significant way. Thus, S does not show a decrease. However, since $\lambda > 1$, then S shows an increase as we lower the temperature, because many beads must adopt the random coil conformation to accommodate the applied strain. In addition, the polymer strands never reach their full elongation.

Fig. 14 shows the heat capacity of the network, C_v, as a function of λ and T. More specifically, what is actually plotted is the change in heat capacity ($\Delta C_v/\phi k_B$), where the reference state is the unstrained network. As expected, the transition temperature (i.e. peak in C_v) increases with increasing strain; larger strains induce the formation of longer helical sequences that are thermodynamically more stable, and thus, require more thermal energy to melt.

Let us now speculate about the effect of chain length. The Wang–Landau algorithm is computationally very intensive. Consequently, only relatively short chains can be simulated, especially if multi-dimensional histograms have to be computed. This limited our study to chains with 30 beads. However, we have also carried out studies of helical polymers using the Wang–Landau algorithm to compute uni-dimensional histograms. The reduced dimensionality of the histograms allowed us to study chains with up to 60 beads. Fig. 6 of the first article in Ref. [13] shows the radial distribution function for a chain with 50 beads. A visual comparison of this figure with Fig. 1 in this article shows that a change in the length of the polymer does not alter the

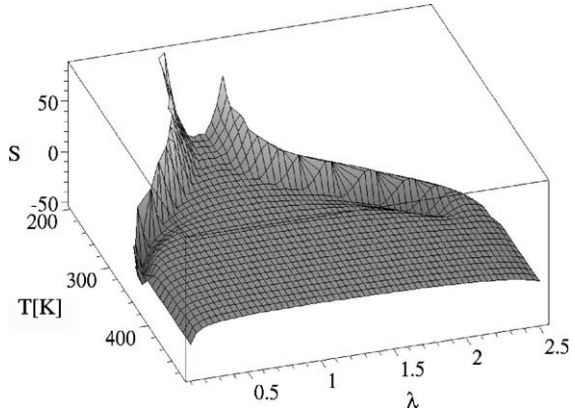

Fig. 13. Network entropy as a function of λ and temperature. As in the case of the single chain, the non-monotonic behavior below the helix-coil transition temperature indicates the induction and melting of helices by mechanical force.

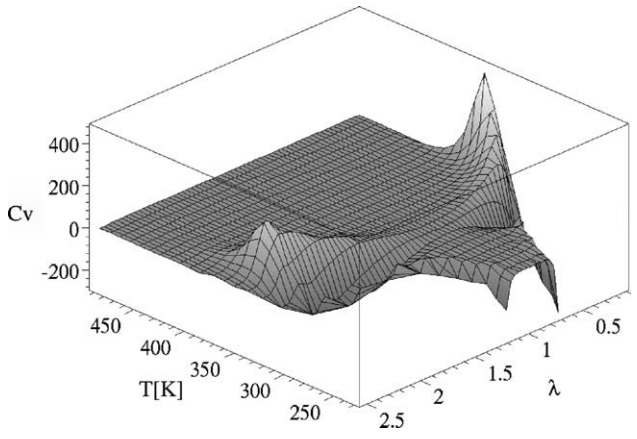

Fig. 14. Network heat capacity as a function of λ and temperature. Analogous to the case of a single chain, the peak indicating a helix-coil transition shifts to higher temperature as elongation of the network increases.

temperature behavior of the radial distribution function in a significant manner. In particular, T_{hc} is almost independent of chain length for chains with more than 20 beads. However, the dependence on R does change. The position of the peak observed at low temperatures changes, as it is expected, because the length of the full helix changes. However, this change is quantitative and not qualitative. This line of reasoning leads us to conclude that a change in the length of the chain will only affect the dependence of the single chain properties, i.e. Figs. 1–7, on temperature and end-to-end distance quantitatively. Similarly, for the case of networks, the qualitative behavior of the various physical properties should not change when the length of the chain changes. Only quantitative changes will occur.

Perhaps, the most important change that could be foreseen is a change in the depth of the minimum in the plots of σ^* vs. λ or T, Fig. 8(b) and (c). As discussed previously, the physical origin of these minima is the increase in the number of random-coil segments by melting of the helical strands due to overstretching or by the increased tendency to form long helical strands as the temperature is reduced. Longer chains would have more segments in the random coil conformation. Therefore, the depth of the minimum should be larger for longer polymers, or, equivalently, it should disappear as the polymer becomes shorter.

4. Conclusions

In this article we have studied the effect of temperature and strain on the properties of an elastomer made of helical polymers. We employed a combination of single-chain Monte Carlo simulations based on the Wang–Landau algorithm and the three-chain model of rubberlike elasticity. The helical polymer was modeled with a modified freely rotating chain model [13].

At the level of a single chain, we found that a decrease in temperature increases the end-to-end distance due to the formation of helical strands, which make the chain stiffer. These strands led to a non-monotonic behavior for the retraction force at low temperatures. Indeed, the retraction force of a chain near or below the transition temperature was found to first increase with increasing end-to-end distance, then decrease, before finally increasing to large values at full extension. Concurrently, the helical content first increases and then decreases to zero for large end-to-end distances. Our study correlated the behaviors of both quantities and, furthermore, showed that the non-monotonic behavior of the force originates from the unraveling of helical strands at large extensions of the chain.

We also explored the dependence of the single-chain entropy on the end-to-end distance at various temperatures. We found that entropy depends on the helical content strongly. In addition, it decreases with increasing end-to-end distance. This facilitates the formation of helices. However, for large extensions, the entropy was found to increase. The heat capacity was found to have a peak that shifts to higher temperatures with increasing end-to-end distance, which indicates that the helix-coil transition temperature increases with increasing end-to-end distance.

As a result of the non-Gaussian behavior of the single chain, we found that the stress–strain relationship of the network shows new features not present in the case of typical elastomers. Specifically, at low temperatures, the network stress first increases, indicating a strengthening of the network, and then decreases before the final increase to very large values due to the finite extensibility of the polymer strands. The decrease for intermediate values of the extension (softening of the network) was proven to be a consequence of the melting of the helical structure by overstretching with respect to the end-to-end distance of the helix. The thermo-elastic behavior of the network proved to be equally unusual, showing a similar variation of stress with decreasing temperature at constant strain.

The helical content was also studied. For this quantity, we found that, except at very low temperatures where the helical content is approximately constant, it increases with increasing strain. This implies a stabilization of the helical conformation by the applied force. However, for large deformations of the network the helical content decreases to accommodate the constraint imposed by the applied strain. This behavior was also seen in the variation of helical content with decreasing temperature at constant strain. We also correlated the behaviors of the helical content and stress, and found that the sharp increase, followed by a decrease, in the stress was due to the melting of the helical strands by the applied strain. This correlation was found both for increasing strain at constant temperature, and for decreasing temperature at constant strain. Further studies of the average number and length of the helical strands shed more light on the mechanisms behind the formation and melting of the helical strands.

The network entropy was found to be controlled by the helical content, decreasing where the latter increases and vice-versa, except at the highest strains and temperatures, where no significant helical content develops. At temperatures far above that of the helix-coil transition, the entropy always decreases with increasing strain. However, at temperatures close to the transition temperature, the entropy first decreases and then increases with increasing strain. This behavior is a consequence of the formation and melting of the helical beads by the applied strain. The heat capacity of the network was found to reach a maximum at higher temperatures for larger strains, indicating an increased helix-coil transition temperature for the network.

In the near future we plan on improving this model by avoiding the use of the Three-chain model. Instead, we will use a finite representation of the network and adapt the Monte Carlo simulation method developed by Escobedo and de Pablo [9] to our system [19].

Acknowledgements

This material is based upon work supported by the National Science Foundation under Grant No. CHE-0132278. Also, acknowledgement is made to The Ohio Board of Regents, Action Fund (Grant#R566).

References

[1] Flory PJ. Principles of polymer chemistry. Ithaca, NY: Cornell University Press; 1953. Mark JE, Erman B. Rubberlike elasticity: a molecular primer. New York: Wiley; 1988. Morawetz H. Polymers: the origins and growth of a science. New York: Wiley; 1985.
[2] Treolar LRG. The physics of rubber elasticity. 3rd ed. Oxford, UK: Clarendon Press; 1975.
[3] Mark JE. Prog Polym Sci 2003;28:1205.
[4] Erman B, Mark JE. Structures and properties of rubberlike networks. New York: Oxford University Press; 1997.
[5] Kuhn WJ. Polym Sci 1946;1:380. Kuhn W. Kolloid Z 1936;76:258. Kuhn W. Angew Chem Int Ed Eng 1938;51:640. James HM, Guth E. Ind Eng Chem 1941;33:624. James HM, Guth E. Ind Eng Chem 1942; 34:1365. James HM, Guth E. J Chem Phys 1943;10:455. James HM, Guth E. J Appl Phys 1944;15:294. James HM. J Chem Phys 1947;15: 651. James HM, Guth E. J Chem Phys 1947;15:669. James HM, Guth E. J Polym Sci 1949;4:153. James HM, Guth E. J Chem Phys 1953;21:1039. Wall FT. J Chem Phys 1942;10:132. Wall FT. J Chem Phys 1942;10:485. Wall FT. J Chem Phys 1943;11:527. Flory PJ. Chem Rev 1944;35:51. Flory PJ. Ind Eng Chem 1946;38:417. Flory PJ. J Chem Phys 1950;18:108. Wall FT, Flory PJ. J Chem Phys 1951;19:1435.
[6] Treolar LRG. Trans Faraday Soc 1946;42:77.
[7] Ronca G, Allegra G. J Chem Phys 1975;63:4990. Graessley WW. Adv Polym Sci 1974;16:1. Ball RC, Doi M, Edwards SF, Warner M. Polymer 1981;22:1010. Edwards SF, Vilgis TA. Polymer 1986;27: 483. Wilder J, Vilgis TA. Phys Rev E 1998;57:5531. Solf MP, Vilgis TA. J Phys I 1996;6:1451. Solf MP, Vilgis TA. J Phys A: Math Gen 1995;28:6655. Vilgis TA, Solf MP. J Phys I 1995;5:1241. Vilgis TA, Erman B. Macromolecules 1993;26:6657. Heinrich G, Vilgis TA. Macromolecules 1993;26:1109. Schimmel KH, Heinrich G. Colloid Polym Sci 1991;269:1003. Rubinstein M, Panyukov S. Macromolecules 2002;35:6670. Rubinstein M, Panyukov S. Macromolecules 1997;30:8036. Rubinstein M, Leiber L, Bastide J. Phys Rev Lett 1992;68:405. Oyerokun FT, Schweizer KS. J Chem Phys 2004;120:9359. Kutter S, Terentjev EM. Euro Phys J E 2001;6:221. Warner M, Terentjev EM. Liquid crystal elastomers. New York: Oxford University Press; 2003.
[8] Duering ER, Kremer K, Grest GS. Phys Rev Lett 1991;67:3531. Grest GS, Kremer K, Duering ER. Europhys Lett 1992;19:195. Grest GS, Kremer K, Duering ER. Physica A 1993;194:330. Duering ER, Kremer K, Grest GS. J Chem Phys 1994;101:8169. Everaers R, Kremer K, Grest GS. Macromol Symp 1995;93:53. Kremer K, Grest GS. In: Binder K, editor. Monte Carlo and molecular dynamics simulations in polymer science. Oxford: Oxford University Press; 1995. p. 194. Grest GS, Putz M, Everaers R, Kremer K. J Non-Cryst Solids 2000;274:139. Heine DR, Grest GS, Lorenz CD, Tsige M, Stevens MJ. Macromolecules 2004;37:3857.
[9] Escobedo F, de Pablo JJ. J Chem Phys 1996;104(12):4788.
[10] Manno M, Emanuele A, Martorana V, San Biagio PL, Bulone D, Palma-Vittorelli MB, et al. Biopolymers 2001;59:51. Manno M, Martorana V, Palma MU. Biophys J 2001;80:1727. Manno M, Emanuele A, Martorana V, San Biagio PL, Bulone D, Palma-Vittorelli MB, et al. Biophys J 2001;80:1743. DeBolt LC, Mark JE. Polymer 1987;28:416. DeBolt LC, Mark JE. J Polym Sci, Part B: Polym Phys 1988;26:865.
[11] Harlepp S, Marchal T, Robert J, Leger J-F, Xayaphoummine A, Isambert H, et al. Eur Phys J E 2003;12:605. Perkins TT, Quake SR, Smith DE, Chu S. Science 1994;264:822. Perkins TT, Smith DE, Chu S. Science 1997;276:2016. Smith SB, Cui Y, Bustamante C. Science 1996;271:795. Rief M, Oesterhelt F, Heymann B, Gaub HE. Science 1997;275:1295. Li HB, Rief M, Oesterhelt F, Gaub HE. Adv Mater 1998;10:316. Kellermayer MSZ, Smith SB, Granzier HL, Bustamante C. Science 1997;276:1112. Rief M, Gautel M, Oesterhelt F, Fernandez JM, Gaub HE. Science 1997;276:1109.
[12] Ferrari F, Cappello J. In: McGrath K, Kaplan D, editors. Protein-based materials. Boston: Birkhäuser; 1997. Petka WA, Hardin JL, McGrath KP, Wirtz D, Tirrell DA. Science 1998;281:389.
[13] Varshney V, Dirama TE, Sen TZ, Carri GA. Macromolecules 2004; 37:8794. Varshney V, Carri GA. Macromolecules 2005;38:780.
[14] Poland D, Scheraga HA. Theory of helix-coil transition in biopolymers. New York: Academic Press; 1970. Bloomfield VA. Am J Phys 1999;67:1212.
[15] Kutter S, Terentjev EM. Eur Phys J E 2002;8:539.
[16] Wang F, Landau DP. Phys Rev Lett 2001;86:2050.
[17] Carri GA, Batman R, Varshney V, Dirama TE. Polymer 2005;46: 3809.
[18] Curro JG, Mark JE. J Chem Phys 1985;82:3820.
[19] Batman R, Carri GA. In progress.